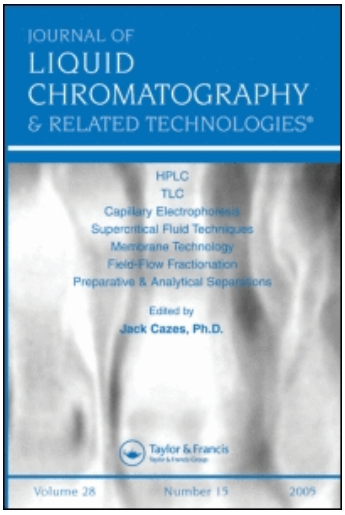

Journal of Liquid Chromatography & Related Technologies
Publication details, including instructions for authors and subscription information:
http://www.informaworld.com/smpp/title~content=t713597273

SEPARATION BEHAVIOR OF BLOOD CELLS IN SEDIMENTATION FIELD-FLOW FRACTIONATION

Yong Jiang; Marcus N. Myers; J. Calvin Giddings‡[a]
[a] Field-Flow Fractionation Research Center, Department of Chemistry, University of Utah, Salt Lake City, UT, U.S.A.

Online publication date: 22 April 1999

To cite this Article Jiang, Yong , Myers, Marcus N. and Giddings‡, J. Calvin(1999) 'SEPARATION BEHAVIOR OF BLOOD CELLS IN SEDIMENTATION FIELD-FLOW FRACTIONATION', Journal of Liquid Chromatography & Related Technologies, 22: 8, 1213 — 1234
To link to this Article: DOI: 10.1081/JLC-100101728
URL: http://dx.doi.org/10.1081/JLC-100101728

J. LIQ. CHROM. & REL. TECHNOL., 22(8), 1213–1234 (1999)

SEPARATION BEHAVIOR OF BLOOD CELLS IN SEDIMENTATION FIELD-FLOW FRACTIONATION

Yong Jiang,[†] Marcus N. Myers,[†,*] J. Calvin Giddings[‡]

Field-Flow Fractionation Research Center
Department of Chemistry
University of Utah
Salt Lake City, UT 84112, USA

ABSTRACT

The separation behavior of red blood cells (RBCs) in sedimentation field-flow fractionation (SdFFF) was investigated under higher field and flow conditions than used previously. This work shows that SdFFF separation of RBCs is fast with the total operating time less than 5 minutes. The resolution is high and the cells retain their integrity after separation. The optimization of cell separation by SdFFF was investigated.

Differences in retention ratios of RBCs from various mammals shows that red cells are separated in the lift-hyperlayer mode based mainly on size differences. Lift forces, especially those originating from deformability and inertial effects play important roles in the separation of red cells and other deformable particles.

INTRODUCTION

Steric and steric/hyperlayer field-flow fractionation (FFF) are particle separation and characterization techniques applicable to particles of 1 to 100 μm in diameter. In steric FFF, particles are driven by the external force to a position nearly in contact with the accumulation wall, from where they commence to migrate downstream. The particle diameter largely determines the migrating velocity. Larger particles, protruding further into the higher flow velocity regions of the channel, are carried downstream more rapidly and thus elute earlier than smaller particles.[1,2] The hyperlayer mechanism is realized when opposing forces exist that are strong enough to drive particles away from the accumulation wall against the external field.[4,5]. If these opposing forces depend on the distance from the channel wall, there are usually some positions where the net force on the particle is zero. A particle will tend to focus at such a position, which may be well removed from the accumulation wall. For cell-sized particles, the principal opposing forces leading to this mode of operation are hydrodynamic lift forces.

FFF has a number of advantages over traditional particle separation techniques. These include high separation resolution, an open channel system, the ease of sample handling, the gentleness of the separation process, flexibility in choice of carrier solution, and the ability to characterize cells, etc., making FFF a useful technique for the separation of biological materials. An important application of steric or steric /hyperlayer FFF is the separation of biological cells.

The feasibility of separating and characterizing cell populations by steric sedimentation FFF (St/SdFFF) was first investigated and demonstrated by its application to fixed human and avian red cells.[5] It was shown that the fixed red blood cells were separated from fresh HeLa cells, which maintained their viability after passing through the separation channel. Giddings et al[6] employed flow FFF for the separation of red blood cells of different origins which were separated based on size differences. The size distributions were determined by using a calibration procedure and were in good agreement with those obtained from Coulter counter analysis. Barman et al[7] further investigated the application of flow/hyperlayer FFF to the separation and size distribution determination of RBCs of diverse size, shape, and origin. They found that the separation is based mainly on the size and shape of the cell particles and that the method is effective both for the separation and characterization of cell populations, including those with cells of abnormal shape and size.

Another important advance in cell separation by FFF was the application of gravitational FFF (GrFFF) to red blood cells. Cardot et al[8,9] used GrFFF for the separation of living blood cells. Merino-Dugay et al[10] employed GrFFF to monitor the composition variation of rabbit RBCs during an experimental

reversible anemia induced by phenylhydrazine. Normal RBCs, the newly produced reticulocytes, and the blood cells containing Heinz bodies showed different retention times in GrFFF. Cardot et al[9,11] further investigated the elution of normal and pathological RBCs in GrFFF by using normal blood cells, sickle cells, and thlassaemic cells. Fractionation of RBCs by GrFFF has also been investigated by Urbankova,[12] who studied the dependence of retention ratio on the flowrate, cell concentration, sample volume, and relaxation time. Recently, the use of a miniature GrFFF channel for RBC separation was reported.[13] These studies demonstrate the following major features of RBCs in a GrFFF channel: (1) Normal RBCs provide a well retained and relatively symmetrical peak. (2) The retention ratio of RBCs increases with flowrate. (3) The retention of RBCs is determined by both the size and density of cells. Retention time and peak shape appeared to be qualitatively related to some biophysical parameters of cells and thus FFF can be a versatile tool for studying cell biophysical characteristics.

Recently, separation and characterization of red blood cells with different membrane deformability using steric sedimentation FFF was reported.[14] Human red blood cells treated by different ways to alter their membrane deformability were studied by SdFFF. Using Sd/stFFF, normal and fixed human red cells were separated with a resolution higher than that from gel permeation. The work showed the deformability of red cells as an important factor influencing lift forces thus the retention behavior of cells. The red blood cells separation behavior in three different FFF systems including gravitational and centrifugal sedimentation FFF were investigated and compared in three independent laboratories, with an objective to determine the relationship between the FFF elution properties and the traditional hematological cell parameters.[15] Negative correlation were found between mean corpuscular volume (MCV) while positive correlation were found between red cell distribution width (RDW) and retention ratios.

Although the potential of FFF for the separation of cells has been well illustrated, there are still some unknown features that need to be investigated. The mechanism of the separation is still not fully understood. Gravitational FFF, although very simple in equipment and convenient in use, requires a long operating time (usually 30 - 60 minutes). In addition, the low field strength of GrFFF limits its resolution, which may become significant when the system is used to investigate the retention mechanism. On the other hand, after many years' of development, sedimentation FFF (SdFFF) has become a very powerful technique for particle separation.[1] Its performance efficiency has been much improved over the system used for the first cell separation work. Using the high field strengths possible with SdFFF, the operating time for cell analysis can be much reduced. In addition, because of the high resolution and variable field strength, SdFFF can provide more precise data for the study of separation mechanisms. In this work, sedimentation FFF was employed to further study

the behavior of RBCs in the FFF channel especially at high flowrate conditions, to further investigate the feasibility of cell separation by FFF, and to search for a better understanding of the separation mechanism of cells and other deformable particles by SdFFF.

Consideration of Retention Mechanisms of Red Blood Cells

It has been shown that in flow FFF, red blood cells are separated in the steric/hyperlayer mode according to volume differences.[6,7] The red cells elute from the channel in such a way that the larger cells exit earlier. With gravitational FFF, the situation is more complicated. In some of early work, the retention ratio was found to be related to cell volume[12] while in other studies this relationship was not observed.[9,11] Instead, cell density has been found to be an important factor influencing retention ratio.[9,11] Other parameters that have been considered as retention influencing factors include cell size and shape, membrane fluidity, and cell deformation. In order to obtain a better understanding of the behavior of red cells in the FFF separation process, in this section, the retention mechanism of red blood cells and other deformable particles in gravitational and sedimentation FFF will be discussed based on a brief review of the literature regarding the motion of deformable particles in shear flow.

In steric FFF, the retention ratio *R*, the ratio of the void time to the particle retention time, is related to particle diameter *d* by:

$$R = \frac{t^0}{t_r} = 3\gamma\frac{d}{w} \qquad (1)$$

where t^0 is the void time or the time that a non-retained component takes to pass through the FFF channel, t_r is the retention time of retained particles, w is the channel thickness, and γ is the steric correcting factor, which is considered to be related to hydrodynamic lift forces and is influenced by flowrate, field strength, and particle size. Equation 1 can be used qualitatively to predict the retention of particles in steric FFF. Due to the complexity of the hydrodynamic lift forces, even for rigid spheres, *R* and *d* usually do not have the linear relationship shown in equation 1. However, the plot of *log R* to *log d* is usually a straight line with a slope slightly smaller than unity. Based on this relationship, a calibration procedure has been established for particle size distribution (PSD) determination.[16] The PSD of particles in the steric size range (1 to 100 μm in diameter) can be determined from their retention ratio and a calibration curve made by using a group of standard particles.

In FFF, two types of hydrodynamic lift forces have been identified: the classic inertial lift force that originates from the inertial effect of fluid and the near-wall lift force, a force that tends to dominate in the near-wall region and which may have its origin in lubrication.[17] The near-wall lift force is proportional to the third power of the particle radius and flow velocity and is inversely proportional to *x*, the distance between the particle and the channel wall. The inertial lift force, on the other hand, is proportional to the fourth power of the particle radius and the second power of the flow velocity. The inertial lift force is also a function of the distance from the channel wall and has three zero-force positions at x/w= 0.19, 0.5, and 0.81, respectively.[18] Without the applied force, the inertial lift force tends to drive all particles toward either of two zero-force positions corresponding to x/w= 0.19, and 0.81 from one of the channel walls. When these lift forces are strong enough and the Brownian motion of particles is negligible, the hyperlayer mode of FFF is realized. Because these lift forces are dependent on the distance between particles and the channel walls and are in the opposite direction to the applied force, particles are focused at a position away from the channel wall where the net force equals zero. The particles thus migrate down the channel at the focused position with a velocity approximately the same as the flow velocity at that position. The retention ratio of the particles now may be expressed as

$$R = 6\left(\frac{x_{eq}}{w} - \frac{x^2_{eq}}{w^2}\right) \qquad (2)$$

where x_{eq} is the position of the particles being focused.

The flow properties of red blood cells are more complicated than those of rigid particles. The motion of red blood cells and other deformable particles in shear flow has been relatively well investigated.[19,20,21] It was found experimentally[21] that at shear rates from 4 to 20 per second in Poiseuille flow, a single red cell rotates as a rigid disc particle. At higher shear rates, the RBC was observed to become aligned with the direction of the flow and to undergo elongation. Experimental work[21,22,23] has also shown that at low Reynolds numbers, where rigid particles do not show significant axial migration, deformable particles will migrate rapidly toward the tube center or toward the region of smallest shape deformation. This inward migration of deformable particles, apparently not arising from inertial effects, has been attributed to the interaction between the drop deformation and the flow field around the particle. It is believed that the fluid drop is deformed by the fluid stresses in a velocity gradient. At equilibrium, the stresses are balanced by interfacial tension. As a result of drop deformation and interaction with the channel wall, a force tending to push the particle away from the wall is generated, leading to drop migration toward the axis.[19] At higher Reynolds numbers rigid spheres exhibit marked

two-way radial migration because of inertial effects, inward from the wall and outward from the tube center. As a result, particles migrate to an equilibrium position. The behavior of normal red cells and hardened red cells at high Reynolds numbers was experimentally compared by Goldsmith,[20] who showed that at a very high shear rate, both types of cells exhibit two-way lateral migration. However, the equilibrium position for normal cells is further displaced toward the axis than it is for the hardened cells.

From these observations, it may be concluded that at low Reynolds numbers, when inertial effects are negligible, deformation is the dominant effect for the inward migration of deformable particles and at high flow rates, both deformation and inertial effects play important roles.

Theoretical studies of the radial migration of deformable particles have also been performed by several researchers.[24,25,26] Although the resultant equations and the calculated lift forces vary with the use of different methods of mathematics and boundary conditions, most results showed that the lift force on a single particle due to deformation is proportional to the second power of flow velocity, the fourth power of the particle diameter, and the deformability of the particle. It is also a function of the ratio of the viscosity of the fluid inside the particle to that of the carrier fluid and the distance of the particle from the tube center.

From the above discussion, it is apparent that a complicated mechanism is involved in the separation of red blood cells (and other biological cells). Once flow is started, the cells will be subjected to lift forces of several origins that tend to drive particles away from the channel wall; these forces are countered by the applied force. Since the lift force due to deformability occurs at very low Reynolds numbers, it may be expected that deformable cells are separated in a hyperlayer mode even at very low flowrates. Because all these lift forces are size dependent, cells will be separated according to size. Unlike in pure steric FFF, where density is not a factor influencing separation as shown in equation 1, in steric/hyperlayer SdFFF or gravitational FFF, density will influence separation because the strength of both gravitational and sedimentation fields are dependent on particle density. Particles of the same size but different densities will be focused at different positions away from the wall, thus being fractionated.

Due to the existence of the extra lift force exerted on deformable particles, it may be expected that for particles of the same volume and density, the more deformable cells will be driven further away from the channel wall. In other words, particles with the same mass but different deformability will show different retention times under the same operating conditions.

EXPERIMENTAL

The sedimentation system used in this work is similar to the S101 SdFFF Colloid/Particle Fractionator (FFFractionation, Salt Lake City, UT). The channel is made by sandwiching a Mylar spacer between two strips of polymethylmethacrylate (PMMA) which provides PMMA channel surfaces. The channel, cut from the Mylar spacer, has dimensions of 87.6 cm in length (tip-to-tip), 0.0254 cm in thickness, and 2.0 cm in breadth. The system rotation rate can be controlled from 10 to 2500±1 rpm, corresponding to field strengths up to 1000 gravities.

An HPLC pump, Kontron model 410 (Kontron Electrolab, London, U.K.) was used for flow-rates below 10 mL/min and an FMI pump model QD-0 (Fluid Metering Inc., Oyster Bay, NY) was used for higher flow-rates. Detection at a wavelength of 254 nm was accomplished using a model 757 UV detector (Applied Biosystem, Ramsey, NJ).

The carrier liquid used was pH 7.2 phosphate buffer saline (PBS) solution containing 10 mM sodium phosphate buffer, 135 mM NaCl, and 0.5 mM EDTA. The osmotic pressure of the carrier solution was measured with a Model 5100 Vapor Pressure Osmometer (Wescor, Logan, UT) and was adjusted to 290 mmol/kg using sodium chloride. All chemicals were obtained from Mallinckrodt Specialty Chemical Co. (Paris, Kentucky).

The human red blood cells were freshly taken from a healthy individual. The animal blood cells used were provided by local animal clinics from healthy subjects. The red blood cells were diluted to 1:40 suspensions in PBS solution and injected directly into the stationary channel through an injection port. The injection volume varied from 2 to 4 µL for different types of cells. Samples were generally injected with a flowrate of 1mL/min for 1 min after which flow was stopped automatically by a model EQ60 valve (Valco Instrument Co. Inc., Houston, TX) for 2 minutes for relaxation and to reach the desired rpm. The flow was then resumed at a specific flowrate as indicated for each run. The data were collected and analyzed by in-lab software.

To avoid overloading, different volumes of the 1: 40 human blood cell samples were injected and fractionated at a field strength of 42 gravities. Testing for overloading was accomplished by comparing the retention times and peak breadths. Overloading was not observed for injection volumes up to 15 µl, which is 5 times more cells than used here. The repeatability of the retention times was tested by running the human blood cells 12 times under the same operating conditions. The average retention time measured at 300 rpm and a flowrate of 15.0 mL/min was 1.35 minutes with a standard deviation of 0.01 minutes.

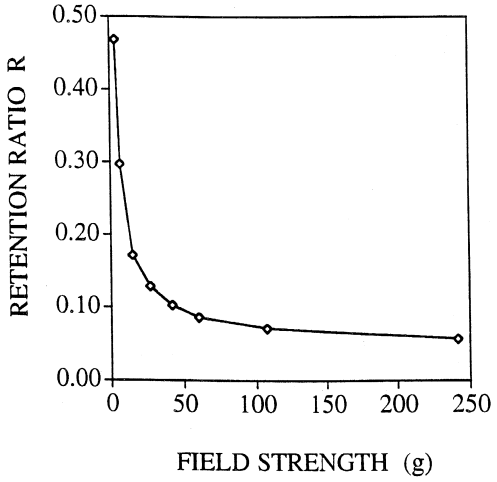

Figure 1. The plot of retention ratio versus field strength for live human red blood cells. The flow velocity was 4.9 cm/sec.

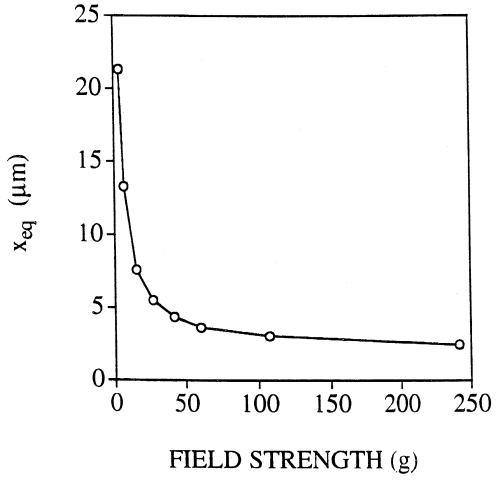

Figure 2. The x_{eq} position of red cells at various field strengths. The flow velocity was 4.9 cm/sec.

RESULTS AND DISCUSSION

Influence of Field Strength and Flow Velocity on Retention

The retention ratio of RBCs at various field strengths was measured at a constant flowrate in order to observe the behavior of RBCs in a SdFFF process. In Figure 1, the measured retention ratios are plotted against field strength. The flowrate used was 14.9 mL/min, corresponding to a flow velocity of 4.89 cm/sec. The figure shows that the retention ratio decreases sharply with the increase in field strength until a relatively constant value is reached. As the field strength was increased from 3.8 to 214 gravities, the retention ratio of human RBCs changed from 0.42 to about 0.05. By using equation 2, the x_{eq} values of the cells under different field strengths were calculated. The results are shown in Figure 2.

The calculated x_{eq} values ranged from about 20 µm to 1.7 µm as the field strength changed from 3.8 to 214 gravities. The shear rate at the wall is around 1000 per second for the flow velocity used and would cause the cells to be elongated and aligned with the flow. The x_{eq} value of 1.7 µm at 214 gravities is still larger than the half thickness of the cells, which has an average value of 0.5 µm. This result indicates that red cells are fractionated in FFF channels in the hyperlayer mode for the field strength range used in this work.

Under the field strength used, the x_{eq}/w value was calculated as from 0.0067 to 0.086. The lift forces in this region are toward the channel center and in the opposite direction to the applied force. Since lift forces are dependent on flow velocity and particle distance from the channel wall (decreasing with increasing distance from the wall), at each field strength particles will be focused at positions where the net force is zero. At higher field strengths, the particles will be driven by the applied force to a position closer to the wall where the lift forces are stronger. On the other hand, when the field strength decreases, the lift forces will drive the particles further away from the channel wall to a new equilibrium position.

It is interesting to compare the behavior of fresh and fixed blood cells. In our work we found that the fresh cells have a shorter retention than the fixed cells which showed the same trend as reported in the literature.[14] We have found under the same operating conditions, the fixed RBCs are always focused closer to the accumulation wall than fresh cells. This shows the extra lift force on deformable particles causes them to stay further away from the channel wall than the rigid particles of the same volume and shape under the same conditions.

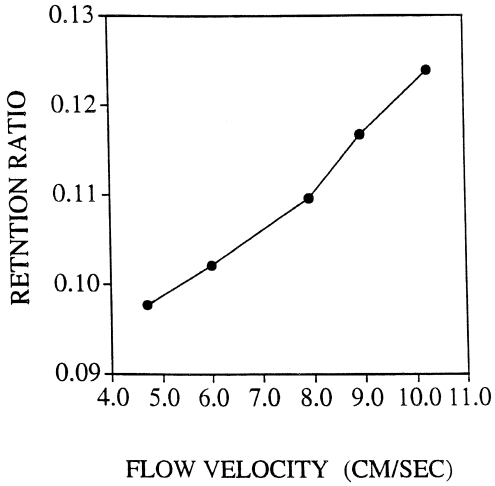

Figure 3. The retention ratios of live red blood cells at various flow velocities. The field strength used was 60 gravities.

The influence of flowrate on the retention ratio of red cells was also observed. Retention ratios were measured at different flow-rates while the field strength was maintained unchanged. As the flow velocity increases, lift forces become stronger and particles are thus driven further into the channel center.

As a result, the retention ratio increases with the increase in flow velocity as shown in Figure 3.

Influence of Operating Conditions on Selectivity and Plate Height

Because of the complexity of the lift forces, it is still impossible to quantitatively analyze how the lift forces influence separation. In this work, selectivity and band broadening are employed as criteria to examine, experimentally, the influence of flow velocity and field strength on cell separation by SdFFF.

Selectivity is a parameter describing the ability of a system to separate materials based on the property of interest. The diameter-based selectivity S_d is defined as:

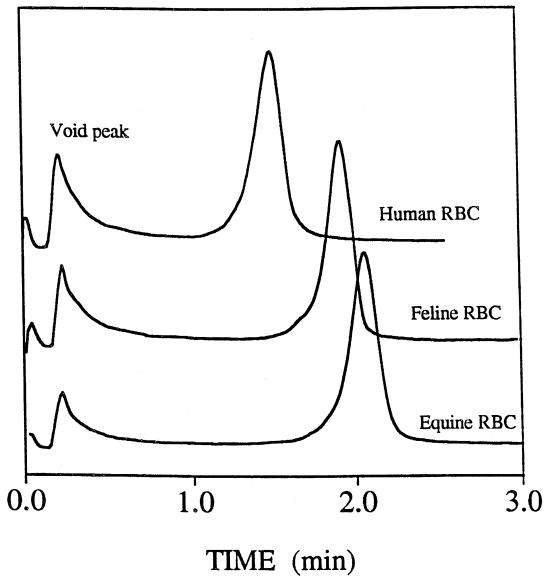

Figure 4. Superimposed fractograms of live red blood cells as indicated. The field strength used was 27 gravities and the flowrate was 14.9 mL/min.

$$S_d = \left|\frac{d\log t_r}{d\log d}\right| = \left|\frac{d\log R}{d\log d}\right| \qquad (3)$$

where t_r is retention time, R is retention ratio, and d is particle diameter. In hyperlayer FFF, selectivity has been found to be influenced by the operating conditions for rigid particles, which is a combination effect of the inertial lift force and the near-wall lift force.

As shown in equation 3, selectivity can be determined by measuring the retention time of cells of different sizes. In the present work, human, feline, and equine blood cells which have different sizes were used. The retention of these three types of cells in sedimentation FFF are shown in Figure 4, which shows canine and human RBC have the shortest retention time corresponding to the largest cell size, while equine RBC has the longest retention time corresponding to the smallest particle size. This result is in accordance with the result in the literature. To determine the selectivity, the diameters of the cells measured by Giddings *et al*[6] using Coulter counter analysis were used.

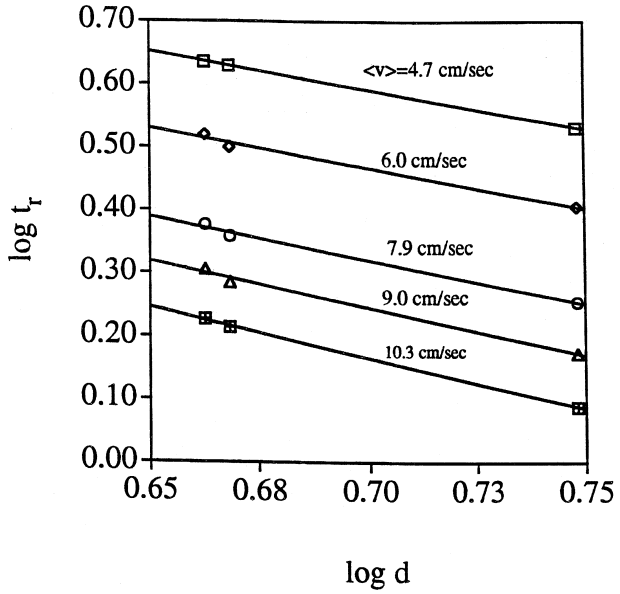

Figure 5. The plot of log t_r vs. log d at various flow velocities. The field strength used was 60 gravities. The three types of live cells used were human RBC, feline RBC and equine RBC from large to small sizes.

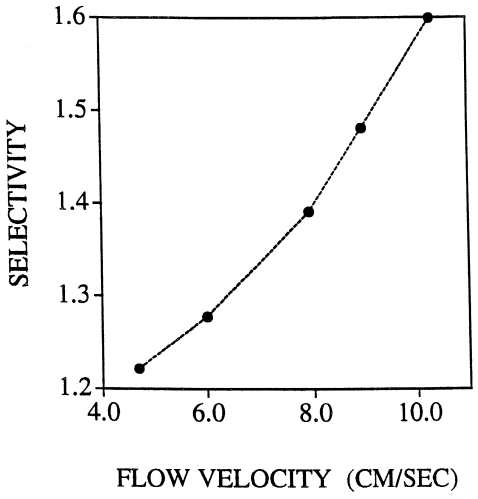

Figure 6. The plot of selectivity vs. flow velocity. The selectivity was calculated from the slope of the log t_r vs. log d plots as shown in Figure 5.

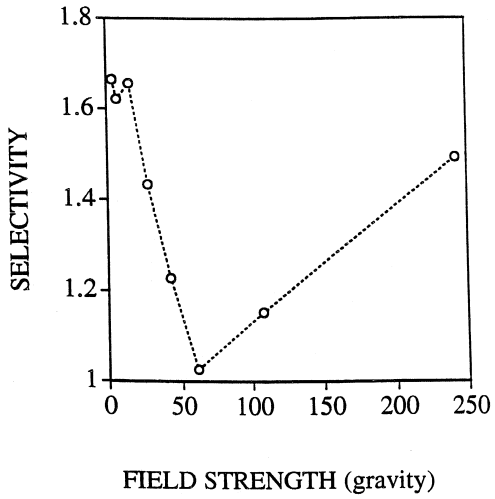

Figure 7. Selectivity at different field strengths.

The diameters of the red cells used in this work may be slightly different from those values in the literature, which will introduce some errors in the determined absolute selectivity values. However, the trend of the selectivity change with flow velocity and field strength will not be influenced by small errors in cell diameters. The retention time at various flowrates and field strengths were measured. Selectivity and plate height at various operating conditions were then calculated. Figure 5 illustrates plots of *log* t_r versus *log d* at different flow velocities. The plots are straight lines and the slope of these lines, which is the selectivity, increases with $\langle v \rangle$. The selectivity calculated from *log* t_r versus *log d* plot in Figure 5 was plotted against $\langle v \rangle$ as shown in Figure 6. As the flow velocity was changed from 4.5 to about 10 cm/sec, the selectivity increased from 1.2 to about 1.6.

The reason for the change of selectivity with flow velocity is rather complicated. The phenomenon has also been observed in steric/hyperlayer FFF of rigid spheres at high flow velocity and relatively low field strength[27] and was explained as the effect of coexistence of near-wall and inertial lift forces, which can be described briefly as follows. For rigid particles, at relatively low flow-rates or high field strength, the balance between the lift forces and the centrifugal force drives particles to a region near the accumulation wall where the near-wall lift force is dominant. Particles are focused in positions such that the distance δ, which is the difference between x_{eq} and particle radius a (the distance between the wall and particles), is identical for particles of all sizes.[17]

The selectivity thus has a value of unity (close to 1 in practical situations). As the flow velocity increases, the inertial lift force (which is proportional to the second power of the flow velocity and fourth power of particle diameter) becomes stronger, driving particles further from the channel wall (where the inertial lift forces are dominating the near-wall lift force). The δ values are no longer identical for particles of different sizes. Instead, large particles are driven further away from the channel wall and the selectivity will be greater than unity.

As discussed in previous section, at high shear flow the total lift force has a two-way nature, changing direction at a certain x position. As a result, the selectivity has unit value at relatively low flow velocity. With an increase in flow velocity, the selectivity starts to increase until a maximum is reached, after which the selectivity will decrease with a further increase in flow velocity. This trend was observed for rigid particles.[27]

For deformable particles, the change of selectivity with $<v>$ should be similar except the lift force due to deformability will play an important role. The lift force due to deformability is also proportional to the second power of flow velocity and the fourth power of particle radius. Consequently, at the same flow velocity and field strength, deformable particles are driven further away from the channel wall. Therefore, selectivity starts to increase at a relatively lower flow rate than that for rigid particles.

In this work, we saw the increase of the selectivity with flow velocity but did not see a maximum under the operating conditions. This could be because with the presence of the lift force due to deformability, the zero force position will shift further into the center of the channel. Under the conditions used, the particles were still far from converging to the zero-force position so that only the part showing increasing selectivity was observed.

Selectivity was also found to change with field strength G as shown in Figure 7. At relatively low field strengths, selectivity decreases with an increase in field strength until a minimum value, after which the selectivity starts to increase with G. The decrease of selectivity with field strength can be explained by the influence of lift forces in the same way as for the change of S with flow velocity. Why the selectivity begins increasing with field strength at relatively high field strengths is not clear. We first assumed that the turning point could be the point at which the longer retained cells were driven in contact with the channel wall while the cells less retained were still suspended.

Once the cells contact the channel wall, they can be further compressed by the increase in field strength, resulting in longer retention. The interaction between the cells and the channel wall could also be a factor.

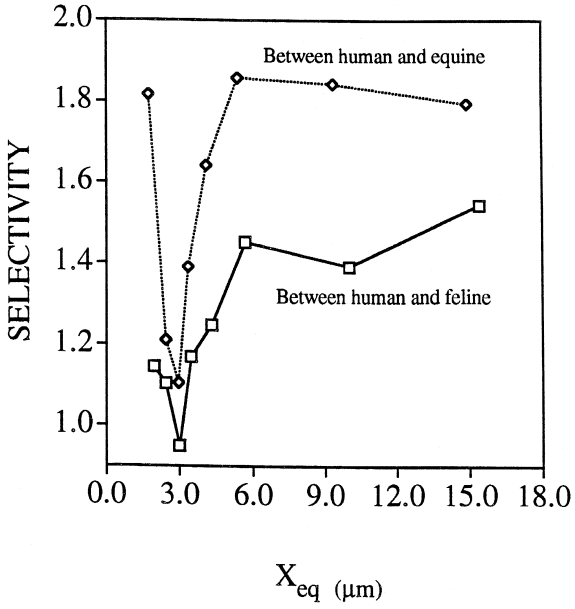

Figure 8. Selectivity between human and equine RBCs at various x_{eq} positions of equine RBC and selectivity between human and feline RBCs at various x_{eq} positions of feline RBC.

For comparison purpose, the selectivity between human and equine RBCs and the selectivity between human and feline RBCs were calculated:

$$S = \frac{\log t_{r1} - \log t_{r2}}{\log d_2 - \log d_1} \qquad (4)$$

where t_{r1} and d_1 are the retention and diameter for the smaller cells while t_{r2} and d_2 are the retention time and diameter for the larger cells.

The selectivity was then plotted against the x_{eq} of the smaller cell (equine RBCs and feline RBCs, respectively).

As shown in Figure 8, both lines reach the lowest point at about 3 μm. At this position, the RBCs have an opportunity to contact the channel wall, if they are tumbling in the channel.

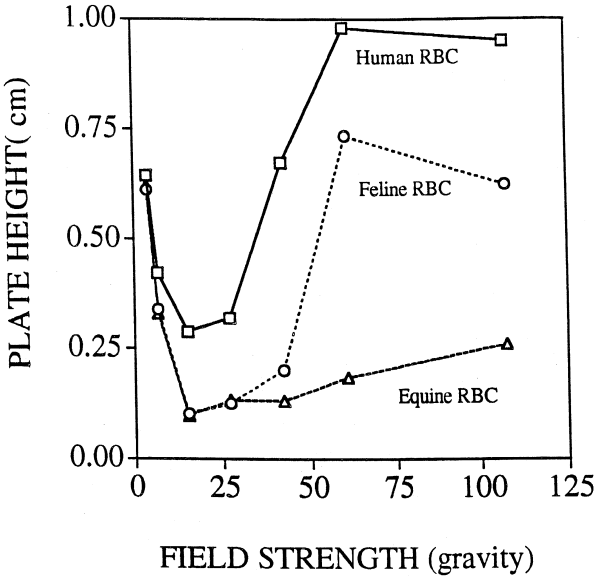

Figure 9. Measured plate heights for the three types of live red blood cells at various field strengths. The flow velocity was 4.9 cm/sec.

The plate height *H* was also found to be influenced by the operating conditions. In Figure 9 the measured plate heights were plotted against field strength. Plate height decreases with the field strength at low field strength, reaches a minimum, and then increases with the field strength.

The response of plate height to flow velocity was also measured and is shown in Figure 10. The plate height decreases with flow velocity within the flowrate ranges of 10 to 32 mL/min.

The present work shows that both selectivity and plate height are influenced by field strength and flow velocity. Selectivity is generally higher for deformable particles than for rigid particles, which means higher resolution may be achieved for deformable particles than for rigid particles. Some of this influence may be explained by lift force theory but is not fully understood yet. It is not possible now to quantitatively predict the optimized conditions for the separation of cells.

The optimized operating conditions can be determined experimentally. Figure 11 shows the fractograms of human and equine RBCs obtained at different field strengths. The best resolution occurred at field strengths of 300 to

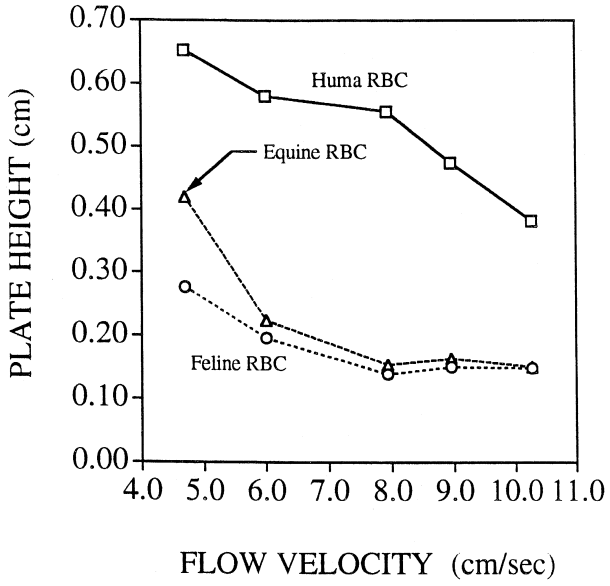

Figure 10. Measured plate heights for the three types of live cells at various flow velocities. The field strength used was 60 gravities.

400 rpm (corresponding to 15.2 and 27 gravities, respectively). At higher or lower field strengths, the resolution became worse. The flowrate used was 14.9 mL/min. It is expected that the field strength for the best resolution differs with flow velocity.

Fractionation of Human RBCs by SdFFF

In order to verify that cell fractionation occurs within a single type of RBCs and that cell integrity is maintained under the high shear conditions used, fractions of human red blood cells were collected at various time intervals and centrifuged for 5 minutes at about 3000 rpm.

The pellets were resuspended in a small volume of carrier liquid, reinjected into the channel, and analyzed under the same conditions as used for the original sample. The fractograms of these reinjected cells are shown in Figure 12. The retention times for the collected fractions fell in the same time intervals in which the fractions were collected. Based on the retention time of the peak maximum, the average cell size for each fraction was determined using a calibration curve constructed from polystyrene latex standards of 5, 7, 10, and 15 µm in diameter.

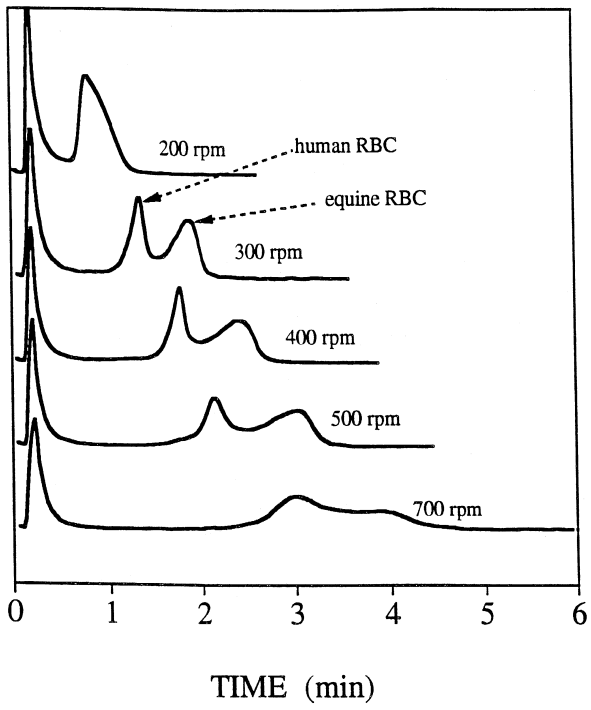

Figure 11. Fractograms of a mixture of live human and equine RBCs at different field strengths. The flow velocity was 4.9 cm/sec.

The diameters of the plate-like red cells in these fractions were also determined using microscopy. Results from the calibration procedure and microscopy are both shown in Table 1, which illustrates that the average sizes of the red cells at different fractions are different. The relatively large standard deviations for both SdFFF sizes and microscope diameters could be the influence of density or deformability.

In Table 1, the SdFFF volume is the volume of spheres that have the same retention time as the red blood cells. We noted that the average volume determined by the calibration procedure was larger than the average volume of human red cells. This is because the extra lift force for deformable particles drives the blood cells further away from the accumulation wall compared to the rigid particles of the same volumes. The deformable cells thus eluted from the channel with the same retention time as that of a much larger rigid particles used to make the calibration curve.

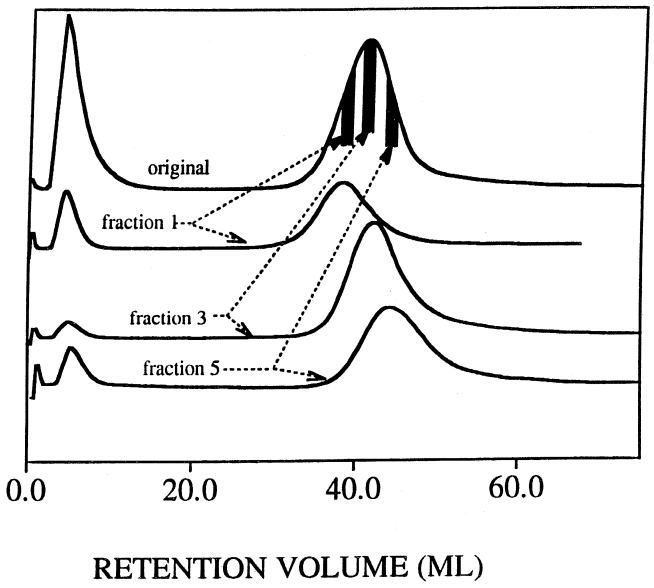

Figure 12. Fractograms of human RBC by Sd/SdFFF. Fractions of the peak of human RBC were collected at various time intervals, concentrated, and reinjected into the channel. The fractograms show the retention of the collected fractions. The field strength was 700m rpm, and the flowrate was 17.1 mL/min.

Table 1

Cell Sizes of Collected Fractions Determined by SdFFF and Microscopy

Fraction #	Retention Time (μm)	SdFFF Diameter (μm)	SdFFF Volume (μm^3)	Diameter by Microscopy* (μm)
1	2.27	7.52±0.84	233±75	8.10±0.48
3	2.50	6.50±0.66	134±44	7.66±0.39
5	2.62	6.06±0.66	109±38	7.55±0.49

* Diameter of disk-shaped red cells under a microscope.

CONCLUSIONS

The existence of the extra lift force for the deformable particles has some important implications on the separation of deformable particles by steric FFF. It may lead to a new mechanism of FFF separation based on the differences in deformability. A drawback is the difficulty understanding cell parameters from the retention data obtained because of the influence of so many factors. The separation is not only based on particle size, but also particle density, shape, and deformability. On the other hand, because deformable cells are driven into the high speed region of the channel, their separation speed is much faster. As shown in this work, the analysis can be accomplished within 1 to a few minutes. Also because of the lift forces, it is possible to use high field strengths that result in high separation resolution. Another related benefit is that, since the cells travel down the channel without touching the walls, there is less possibility they will interact with or adhere to the channel surfaces, which will help to maintain the cell properties, avoid cell loss in the channel, and prevent the channel surface change caused by the adsorption of cells.

REFERENCES

† Present address: FFFractionation LLC, Salt Lake City Utah, USA.

‡ Deceased November 26, 1996.

1. J. C. Giddings, Science,**260**, 1456 (1993).

2. K. D. Caldwell, Anal. Chem., **60,** 959A (1988).

3. T. Koch, J.C. Giddings, Anal. Chem., **58**, 994 (1986).

4. J. C. Giddings, Sep. Sci. Technol., **18,** 765 (1983).

5. K. D. Caldwell, Z. Q. Cheng, P. Hradecky, J. C. Giddings, Cell Biophysics, **6**, 233 (1984).

6. J. C. Giddings, B. N. Barman, M. K. Liu, in **Cell Separation Science and Technology** (ACS Symposium Series, No. 464), D. S. Kompala, P. Todd, eds., American Chemical Society, Washington, DC, 1991, pp.128.

7. B. N. Barman, J. C. Giddings, Anal. Biochem., **212**, 35 (1993).

8. A. Bernard, B. Paulet, V. Colin, Ph. J. P. Cardot, Trends in Anal. Chem., **14**, 256 (1995).

9. Ph.J. P. Cardot, J. Gerota, M. Martin, J. Chromatogr., **568**, 93 (1991).

10. A. Merino-Dugay, Ph. J. P. Cardot, M. Czok, M. Guernet, J. P. Andreux, J. Chromatogr., **579**, 73 (1992).

11. Ph. J. P. Cardot, C. Elgea, M. Guernet, D. Godet, J. P. Andreux, J. Chromatogr. B, **654**, 193 (1994).

12. E. Urbankova, A. Vacek, N. Novakova, F. Matulik, J. Chmelik, J. Chromatogr., **583**, 27 (1992).

13. V. Yue, R. Kowal, L. Neargarder, L. Bond, A. Muetterties, R. Parsons, Clin. Chem., **40**, 1810 (1994).

14. X. Tong, K. D. Caldwell, J. Chromatogr B, **674**, 39 (1995).

15. R. Parsons, V. Yue, X. Tong, P. Cardot, A. Bernard, J. P. Andreux, K. Caldwell, J. Chromatogr B, **686**, 177 (1996).

16. J. C. Giddings, M. H. Moon, P. S. Williams, M. N. Myers, Anal. Chem., **63**, 1367 (1991).

17. P. S. Williams, T. Koch, J. C. Giddings, Chem. Eng. Comm., **111**, 121 (1992).

18. P. S. Williams, S. Lee, J. C. Giddings, Chem. Eng. Comm., **130**, 143 (1994).

19. H. L. Goldsmith, Federation Proceedings, **26**, 1813 (1967).

20. H. L. Goldsmith, Federation Proceedings, **30**, 1578 (1971).

21. H. L. Goldsmith, S. G. Mason, J. Colloid Sci., **17**, 448 (1963).

22. A. Karnis, H. L Goldsmith, S. G. Mason, Nature, **200**, 159 (1963).

23. A. Karnis, S. G. Mason, J. Colloid Science, **24**, 164 (1967).

24. C. E. Chaffey, H. Brenner, S. G. Mason, Rheol. Acta, **4**, 56 (1965).

25. Philip R. Whol, S. I. Rubinow, J. Fluid Mech., **62**, 185 (1974).

26. P. C.-H. Chan, L. G. Leal, J. Fluid Mech., **92**, 131 (1979).

27. Y. Jiang, **Studies in Field-Flow Fractionation**, Ph. D. Thesis, University of Utah, Salt Lake City 1994, Ch. 3.

Received November 11, 1997
Accepted January 14, 1998
Manuscript 4646